Percutaneous ablation of obscure hypovascular liver tumours in challenging locations using arterial CT-portography guidance

V. Schembri, L. Piron, J. Le Roy, M. Hermida, J. Lonjon, L. Escal, M.-A. Pierredon, A. Belgour, C. Cassinotto, B. Guiu

Percutaneous ablation of obscure hypovascular liver tumors in challenging locations using arterial CT-portography guidance

Short Title:

Thermal ablation using CT-portography guidance

V. Schembri[a], L. Piron[a], J. Le Roy[b], M. Hermida[a], J. Lonjon[a], L. Escal[a], M.-A. Pierredon[a], A. Belgour[a], C. Cassinotto[a] , B. Guiu[a*]

[a] Department of Radiology, St-Eloi University Hospital, 34980 Montpellier, France
[b] Department of Radiation Protection, University Hospital, 34980 Montpellier, France

***Corresponding author** : B-guiu@chu-montpellier.fr

Abstract

Purpose The purpose of this study was to evaluate the feasibility, safety and efficacy of percutaneous ablation (PA) of obscure hypovascular liver tumors in challenging locations using arterial CT-portography (ACP) guidance.

Materials and methods. A total of 26 patients with a total of 28 obscure, hypovascular malignant liver tumors were included. There were 18 men and 6 women with a mean age of 58 ± 14 (SD) years (range: 37 – 75 years). The tumors had a mean diameter of 14 ± 10 (SD) mm (range: 7 – 2 4 mm) and were intrahepatic cholangiocarcinoma (4/28; 14%), liver metastases from colon cancer (18/28; 64%), corticosurrenaloma (3/28; 11%) or liver metastases from breast cancer (3/28; 11%). All tumors were in challenging locations including subcapsular (14/28; 50%), liver dome (9/28; 32%) or perihilar (5/28; 18%) locations. A total of 28 PA (12 radiofrequency ablations, 11 microwave ablations and 5 irreversible electroporations) procedures were performed under ACP guidance.

Results. A total of 67 needles (mean: 2.5 ± 1.5 [SD]; range: 1 – 5) were inserted under ACP guidance, with a 100% technical success rate for PA. Median total effective dose was 26.5 mSv (IQR: 19.1, 32.2). Two complications were encountered (pneumothorax; one abscess both with full recovery), yielding a complication rate of 7%. No significant change in mean creatinine clearance was observed (80.5 mL/min at baseline and 85.3 mL/min at day 7; P = 0.8). Post-treatment evaluation of the ablation zone was overestimated on ACP compared with conventional CT examination in 3/28 tumors (11%). After a median follow-up of: 20 months (range: 12 – 35 months), local tumor progression was observed in 2/28 tumors (7%).

Conclusion. ACP guidance is feasible and allows safe and effective PA of obscure hypo-attenuating liver tumors in challenging locations without damaging the renal function and with acceptable radiation exposure. Post-treatment assessment should be performed using conventional CT or MRI to avoid size overestimation of the ablation zone.

Keywords: CT portography; Percutaneous treatment; Microwaves; Carcinoma, hepatocellular; Liver neoplasms

Abbreviations

CT: computed tomography; DAP: Dose area product; DLP: dose-length product; ED: effective dose; HCC; hepatocellular carcinoma; IRE: irreversible electroporation; LTP: Local

tumor progression; MRI: magnetic resonance imaging; MWA: microwave ablation; PA: percutaneous ablation; SIR: society of interventional radiology; SMA: superior mesenteric artery

Introduction

Percutaneous ablation (PA) is a minimally invasive technique routinely performed for the treatment of small-sized primary or secondary liver tumors [1-4]. PA alone or in combination with surgery can effectively treat liver metastases with an excellent safety profile and a low rate of complications [5-7]. Ultrasound remains the most commonly-used guidance modality, owing to its wide availability and its real-time imaging ability without any radiation exposure. However, many lesions are not visible under ultrasound, especially since they are small, or due to pleural or bowel interposition [7, 8]. In these cases (*i.e.*, the so called "obscure lesions"), lesion targeting may require computed tomography (CT) guidance or fusion technologies. However, small liver tumors are rarely spontaneously visible on unenhanced CT and metal streak artifact of the ablation probe impairs even more the visibility of the lesion [9]. Some solutions have been proposed to keep the lesion visible all along the procedure. For hypervascular liver tumors like hepatocellular carcinomas (HCC) or neuroendocrine tumors, intra-arterial injection of ethiodized oil allows persistent tumor tagging [10]. Unfortunately, such approach does not work for non-hypervascular tumors, such as colon metastasis or intrahepatic cholangiocarcinoma. These tumors become visible as hypoattenuating nodules at CT during the portal phase, but only transiently which does not allow for accurately inserting needle(s) in most procedures. To avoid a drift to palliative treatments in such situations, van Tilborg et al. proposed the use of arterial CT-portography to make the tumor visible using a small amount of contrast medium, making possible to inject several times through the superior mesenteric artery (SMA) to guide needle(s) [11]. In their study, the patient needed to be transported from the angio-suite to the CT-suite, which may be complex for logistical reasons. The recent availability of angio-CT suites clearly facilitates such multimodal approaches in daily practice [12]. In such environment, arterial CT-portography represents an attractive way to target obscure tumors especially when they are in challenging location (subcapsular, dome, centrally-located) where high accuracy of needle placement is required.

The purpose of this study was to evaluate feasibility, safety and efficacy of PA of obscure hypovascular liver tumors in challenging location using arterial CT-portography guidance.

Materials and methods

Study design

This retrospective study was performed using data prospectively collected in a database of patients who underwent liver PA at our institution. This study was performed in accordance with the Declaration of Helsinki and approved by our Institutional Review Board. Written informed consent for the procedure and anonymous data collection was obtained from all patients prior PA.

Inclusion criteria were: invisible tumor under ultrasound and unenhanced CT examination; tumor size ≤ 30 mm; WHO performance status 0 or 1; prothrombin time ratio > 50%; and platelet count > 5×10^9/L. Exclusion criteria were HCC or neuroendocrine metastases; extrahepatic metastases or macrovascular invasion; imaging follow-up of less than one year; history of biliary-digestive anastomosis or endoscopic sphincterotomy; combined treatment with embolization or chemoembolization; renal failure (*i.e.*, creatinine clearance < 40 mL/min). Treatment was validated during a multidisciplinary meeting that included interventional radiologists, liver surgeons, oncologists, hepatologists and radiation oncologists. All patients underwent contrast-enhanced multiphase CT and/or magnetic resonance imaging (MRI) (including dynamic MRI) within 1 month prior PA. All patients were seen in consultation by an interventional radiologist. Laboratory tests were systematically performed to detect any possible contraindication to PA.

PA procedure

All PAs were performed in a multimodality angio-CT suite (Infinix-I 4D CT® system, Canon Medical Systems) by four interventional radiologists with 5 to 15 years of experiencein hepatic tumor PA. Patients were placed in supine position with arms above the head when possible. All procedures were done under general anesthesia with endotracheal intubation. Patients were mechanically ventilated using low tidal volume ventilation (i.e., tidal volume between 3 to 4 mL/kg and > 320 mL/min) to strongly limit liver movements [13]. Respiratory rate was adjusted to maintain the end tidal carbon dioxide between 35 and 45 mmHg.

For non-centrally located tumors, PA was performed using radiofrequency ablation (RFA) or microwave ablation (MWA) depending on the operator choice. For perihilar lesions, irreversible electroporation (IRE) was used. RFA was performed using a separable clustered internally-cooled (Octopus®, STARmed) electrode with one, two or three electrodes. When

two or three electrodes were needed, the generator (VIVA MultiR®, STARmed) was used in dual-switch mode. MWA was performed using a single 15G internally-cooled electrode (Acculis MTA system®, Angiodynamics). For IRE, we used the Nanoknife system (Angiodynamics, Amesterdam) with 4 – 6 needles to administrate 90 pulses (70µs per pulse; 1,200 – 2,000 V/cm to obtain approximately 30 A between each couple of needles; 1.2 – 2.2cm electrode distance; active tip, 2.5cm). Whatever the technique, the objective was to completely ablate the tumor(s) with a 5mm-1cm margin. For RFA/MWA, needle track ablation was performed according to the manufacturer's instructions. Hydro (5% dextrose) or CO_2 dissection was used whenever necessary to protect the surrounding organs against thermal injury [14].

Arterial CT-portography guidance

The arterial CT-portography was using a 5-F sheath introduced in the right common femoral artery. Then, a 5-F Simmons 1 catheter (Terumo) was used to catheterize the superior mesenteric artery (SMA) with the tip at the proximal part. For tumors located in the liver dome, the extrapulmonary transthoracic transdiaphragmatic route was used after artificially induced pneumothorax with CO_2 [13, 15]. First, two CT volume acquisitions on the liver were performed following intra-arterial administration of iodinated contrast material in the SMA using the following parameters: sequential acquisition (one rotation); total collimation, 320 × 0.5 mm; rotation time, 0.35 s; slice thickness, 0.5 mm; kV, 120; tube current, 80-500 mA with automatic tube current modulation (noise index: 9.5); volume of contrast medium, 25 mL (Xenetix® 350; Guerbet); flow rate, 4 mL/s; scan delay, 30 s and 40 s. Depending on patient hemodynamic, the acquisition providing the best tumor-to-liver contrast (at 30 s or 40 s) was assessed for treatment planning. Second, needle placement was performed under CT-fluoroscopy guidance (120 kV, 100 mAs, 4-mm slice thickness) while repeating on demand contrast injection in the SMA. For each contrast injection in the SMA, operator had a 20 – 30 s interval time to repeat CT-fluoroscopy and place the needle(s). For all procedures, we fixed an upper limit of 2 mL/kg of injected contrast material for the whole procedure to prevent any subsequent renal failure. Fluoroscopy time, number of CT and fluoroscopy acquisitions, dose-length product (DLP) and total dose-area product (DAP) were gathered. Effective doses (ED) were obtained using validated conversion factors [16, 17].

Follow-up

CT examination was systematically performed at the end of the procedure in order to evaluate the ablation zone (*i.e.*, the area of low attenuation) and to detect post-procedural complications. Technical success was defined as complete ablation of the target tumor(s) [18].

Depending on the amount of contrast medium used for needle guidance, arterial CT-portography (25 mL of pure iobitridol at a concentration of 300 mg of iodine per mL) was performed and/or regular CT examination at the portal phase (70 s after intravenous injection of 70 mL of contrast medium, 3 mL/s) was acquired whenever possible, to check for mismatch between both examinations. When the amount of 2 mL/kg was reached for needle guidance, only unenhanced CT images were used to check for complication. Hepatic MRI examination was performed within the following two days.

The type and number of complications were recorded and classified according to the Society of Interventional Radiology (SIR) guidelines [18]. Patients were monitored overnight. All patients underwent a clinical examination and laboratory tests the day after PTA. Then, patients were evaluated using MRI (including dynamic acquisitions and diffusion-weighted sequence) at 4 – 6 weeks following the procedure and then every 3 months. Local tumor progression (LTP) was defined by any growing or tumor focus within or at the edge (direct contact) of the ablation zone, after complete ablation documented by at least one MRI examination [19].

Statistical analysis

Continuous variables were expressed as means ± SD and ranges or medians with interquartile ranges (IQR) and ranges, and categorical variables as raw numbers, proportions and percentages. Comparison between baseline and follow-up creatinin clearance values were performed using Wilcoxon signed-rank test. All analyses were performed with the Stata software, version 16.0 (Stata corporation, College Station, TX, USA). A P-value <0.05 was considered significant.

Results

Patients and tumors characteristics

Between September 2017 and July 2019, 242 PTA of liver tumors were performed in 156 patients at our institution. Twenty-eight PA procedures performed in 26 patients with a total

of 28 tumors met inclusion criteria for this study **(Figure 1)**. There were 18 men and 8 women with a mean age of 58 ± 14 (SD) years (range: 37 – 75 years) No patients had underlying liver cirrhosis. Tumor characteristics and procedure details are shown in **Table 1**. Tumor nodules were subcapsular (14/28; 50%), located at liver dome (9/28; 32%) or centrally-located adjacent to the hepatic hilum (5/28; 18%)). Their mean diameter was 14 ± 10 (SD) mm (range: 7 – 24 mm). The nature of liver tumors was hepatic metastasis from colon cancer (18/28; 64%), intrahepatic cholangiocarcinoma (4/28; 14%), corticosurrenaloma (3/28; 11%) or metastasis from breast cancer (3/28; 11%). Eight patients (8/26; 31%) were treatment-naïve regarding their liver tumor) and eight patients had prior liver therapies such as PA (4/28; 14%), surgical resection (3/28; 11%) and surgical resection combined with PA (1/28; 4%).

Two patients (2/26; 8%) were ASA 3, whereas the others were ASA 1-2. Mean platelet count was 183,000 ± 68,000 (SD) /mm^3 (range: 72,000 – 264,000/mm^3) and mean prothrombin time was 95 ± 7 (SD) % (range: 85 – 100%). Mean baseline creatinine clearance was 80.5 ± 21.2 (SD) mL/min (range: 59 – 107 mL/min).

PA techniques

All tumors were clearly visible on arterial CT-portography in all procedures **(Figure 2)**. A total of 67 needles (mean: 2.5 ± 1.5 [SD]; range: 1 – 5) were inserted under arterial CT-portography to ablate all liver tumors. Multiple needle insertions were required during the procedure in 19 patients (19/26; 73%). RFA and MWA were used in 12 (12/28; 43%) and 11 (11/28; 39%) tumors, respectively whereas IRE was performed to treat the remaining five tumors (5/28; 18%). Artificial CO2 pneumothorax with CO_2 was necessary in 9/28 (32%) PA procedures. In three PA procedures (3/28; 11%), hydro-dissection of a proximal organ was used to prevent thermal damage.

For angiography, mean fluoroscopy time was 163 ± 24 (SD) s (range: 15 – 382 s). The mean number of CT and CT-fluoroscopy acquisitions were 5.5 ± 3.5 (SD) (range: 3 –14 s) and 44 ± 11 (SD) (range: 8 – 149), respectively. Median DLP, DAP and ED are reported in **Table 2.** CT was responsible from 98% of total ED.

Adverse events

No peritoneal bleeding, pleural bleeding or femoral access complication was observed. Only 2 SIR grade C complications were encountered in two procedures in two different patients, resulting in a 7% complication rate. One patient had an iatrogenic pneumothorax following

PTA of a cholangiocarcinoma located at the hepatic dome, treated at the end of the procedure by a 7-F drain placed percutaneously in the pleural space connected to a negative-pressure aspiration system for 24 hours. This patient fully recovered and was discharged at day 3. The second complication was an abcess formation at the ablation zone, 10 days following IRE of intrahepatic cholangiocarcinoma. Complete resolution was observed after percutaneous aspiration and IV antibiotic administration for 7 days. Except for these two patients, hospital stay was 2 days.

Follow-up

Technical success was obtained in all tumors (28/28; 100%) based on arterial CT-portography performed at the end of the PA procedure (20/28; 71%), on liver MRI at day 1 (5/28; 18%), and on abdominal CT examination (portal phase) in addition to immediate arterial CT-portography (3/28; 11%). In all patients undergoing both examinations (3/28; 11%), discordances were observed when comparing arterial CT-portography and CT examination features regarding the size of the ablation zone (*i.e.,* hypoattenuating area) that was overestimated on arterial CT-portography **(Figure 3)**.

Mean creatinine clearance changed from 80.5 mL/min at baseline to 85.3 mL/min at day 7, with no significant difference (P = 0.8). During a median follow-up of 20 months (range: 12 - 35 months), LTP was observed in only two tumors (2/28; 7%). However, 15 patients (15/26; 58%) presented with intrahepatic distant (12/15; 80%) or extra-hepatic recurrence (3/15; 20%).

Discussion

In this study, we describe the technical details, results and outcomes of patients treated by PTA using arterial CT-portography guidance in a multimodal suite. Our results confirm that arterial CT-portography represents an attractive way to target obscure hypovascular tumors especially when they are in challenging location where high accuracy of needle placement is required. Both feasibility and safety of PA under arterial CT-portography guidance were ensured despite a vast majority (73%) of patients needing insertions of multiple needles. No puncture-related complication was noticed. Excellent oncological results were observed since only 7% of LTP was reported after a long follow-up (median, 20 months) of at least 12 months per tumor, whereas the best LTP results of PA for liver metastases are usually approximately of 10% in the literature [7, 20, 21].

Ultrasound is the modality of choice for guidance of PA given its wide availability, real-time and radiation-free imaging capability. Hypoattenuating lesions such as colorectal liver metastases or intrahepatic cholangiocarcinoma are challenging to ablate when they are invisible under ultrasound. In such situations, CT guidance can be used but such tumors are generally not visible at unenhanced CT as well. PA based on anatomical landmarks is then an option but due to both heterogeneous stiffness of hepatic structures and liver deformation during respiratory movements or needle insertion, such "blind" approach carries a risk of unprecise targeting and by the way, either a high risk of incomplete ablation or a high rate of LTP due to inadequate ablation margins. At contrast-enhanced CT, such tumors can become visible but only transiently, making precise needle insertion very challenging or even impossible, especially when multiple needles are required. ultrasound/CT fusion imaging has been proposed [22, 23] with a spatial accuracy ranging between 1.9 – 19.1 mm depending on how the patient is ventilated and when CT examination used for fusion has been performed. Potential discrepancies between real and virtual coordinates of the needle positioned using ultrasound/CT fusion may be problematic for PA [22], especially when tumor location is challenging (subcapsular, close to other organs, large vessels or bile ducts) or in case of at-risk structures nearby the target. The same applies to electromagnetic navigation system, even when combined with high-frequency jet-ventilation since mean tip-to-tumor distance has been reported at 22 mm [24].

Because accurate intra-procedural targeting is highly desirable to achieve complete PA with adequate margins, arterial CT-portography has been proposed for PA guidance of obscure tumors [11]. Arterial CT-portography is an old technique for detecting liver metastases, based on portal enhancement of the liver by infusion of contrast material through the SMA. The rationale relies on the maximized liver-to-lesion attenuation difference, as a consequence of an almost exclusive arterial blood supply of the liver tumors, contrary to the surrounding liver parenchyma [25]. Of note, arterial CT-portography may have limited sensitivity for primary liver tumors, and especially for those developing on underlying chronic liver disease [26].

To our knowledge, CT-portography as a guidance tool was first proposed by van Tilborg et al. in a series of 31 hepatic tumors [11]. In their study, the patient needed to be transported from the angio-suite to the CT-suite, thereby limiting a widespread use. The recent availability of angio-CT suites is an excellent opportunity to incorporate this technique in daily clinical practice for obscure liver tumors, especially when a careful needle placement is required [12].

CT-fluoroscopy guidance usually makes difficult to place the needle accurately in the z-axis, which can result in cranio-caudal errors [9, 27] due to respiratory movements. In our series, the ability to visualize 100% of these small tumors was also facilitated by limiting the respiratory motion with low tidal volume ventilation as proposed elsewhere [28]. Contrary to what was reported by Stattaus et al. [29], we did not encountered problematic streak artefact due to metallic probes, probably because we mainly used 17-G probes and lesion-to-liver contrast provided by arterial CT-portography was high enough to see and reach the tumors.

Besides differences in tumor characteristics (smaller lesions in our study) and ablation techniques (multi-needle ablation in most of our patients) as compared to the study by van Tilborg et al [11], we used a slightly different injection technique. In this regard, 25 mL of pure contrast-medium were injected and imaging was started at 30 s or 40 s after injection, whereas Tilborg et a. used 20 mL of iodinated contrast material mixed with 40 mL of saline with a shorter delay (18 s) for starting scanning. The best protocol remains to be determined but contrary to van Tilborg et al. [11], we did not observe any gravity-induced gradient in contrast concentration described as highest liver-lesion contrast in dorsal liver segments for patients in supine position. Greater iodine concentration and later imaging in our protocol probably better compensated for incomplete mixing in the portal vein of densely contrasted blood from the SMA and non-contrasted blood from the splenic vein. Repeated injection of lower amounts of fluid also prevents to increase too much cardiac pre-charge.

In our study, we found a significant difference in the post-treatment assessment of the ablation zone in the three patients where we did both immediate post-treatment arterial CT-portography and conventional CT during the portal phase. Whether it is well known that arterial CT-portography can show false-positive lesion positive (focal steatosis, benign tumors, physiological variation in portal perfusion) [30], justifying to target only tumors previously depicted on standard imaging (CT or MRI examination), the ablation zone was clearly overestimated on arterial CT-portography in the three patients who underwent both examinations for comparison. We can hypothesize that portal perfusion was impaired (compression or thrombosis of small portal venules) in the peri-ablation zone and/or along the needle path. Therefore post-treatment evaluation should not be performed using arterial CT-portography, but rather using conventional CT/MRI imaging.

In our study, we did not observe any renal function worsening by keeping the amount of iodinated contrast material below 2 mL/kg. It was enough to identify all tumors, even with multiple needle insertions including for IRE of central tumors for which needle placement

may be complex. Finally, radiation exposure delivered to the patient and the staff must be in accordance with the ALARA principle [31, 32]. Radiation exposure resulting from SMA catheterism was negligible as compared to CT-induced radiation, estimated by a median 1727mGy.cm DLP. Noteworthy, CT-induced radiation was within the range of what was previously published for percutaneous liver tumor ablations (**Table 3**) [33-35].

Several limitations to this study must be acknowledged: first, this a retrospective, single center study with limited sample size and heterogenous PA treatments (RFA, MWA, IRE) but we focused on obscure hypovascular tumors in difficult locations to address an important issue in daily practice, that may result to switch for palliative therapy with subsequent loss of chance for the patient. Second, spatial accuracy of needle placements was not evaluated because we did not routinely perform arterial CT-portography with the needles in place, in order to limit radiation exposure and keep the possibility to perform post-procedure arterial CT-portography or portal CT examination to evaluate the ablation zone. However, we made the choice to report on clinically-meaningful endpoints, including feasibility, safety and oncological outcome by evaluating LTP with at least 12-month follow-up.

In conclusion, arterial CT-portography guidance in a multimodal suite is feasible and allows effective percutaneous ablation of obscure hypovascular liver tumors in challenging locations without significant impact on the renal function and with acceptable radiation exposure. However, immediate post-treatment assessment of the ablation zone using arterial CT-portography seems overestimated, which is in favor for treatment evaluation using conventional CT or MRI.

Human rights

The authors declare that the work described has been carried out in accordance with the Declaration of Helsinki of the World Medical Association revised in 2013 for experiments involving humans.

Disclosure of interest

The authors declare that they have no competing interest.

Funding

This work received no funding.

Author contributions

All authors attest that they meet the current International Committee of Medical Journal Editors (ICMJE) criteria for Authorship.

REFERENCES

[1] Choi D, Lim HK, Rhim H, Kim YS, Lee WJ, Paik SW, et al. Percutaneous radiofrequency ablation for early-stage hepatocellular carcinoma as a first-line treatment: long-term results and prognostic factors in a large single-institution series. Eur Radiol 2007;17:684-92.

[2] Vroomen L, Petre EN, Cornelis FH, Solomon SB, Srimathveeravalli G. Irreversible electroporation and thermal ablation of tumors in the liver, lung, kidney and bone: What are the differences? Diagn Interv Imaging 2017;98:609-17.

[3] Takai Takamatsu R, Okano A, Yamakawa G, Mizukoshi K, Obayashi H, Ohana M. Impact of an ultrasound-guided radiofrequency ablation training program on the outcomes in patients with hepatocellular carcinoma. Diagn Interv Imaging 2019;100:771-80.

[4] Young S, Rivard M, Kimyon R, Sanghvi T. Accuracy of liver ablation zone prediction in a single 2450MHz 100 Watt generator model microwave ablation system: an in human study. Diagn Interv Imaging 2020;101:225-33.

[5] Cirocchi R, Trastulli S, Boselli C, Montedori A, Cavaliere D, Parisi A, et al. Radiofrequency ablation in the treatment of liver metastases from colorectal cancer. Cochrane Database Syst Rev 2012:CD006317.

[6] Minami Y, Nishida N, Kudo M. Radiofrequency ablation of liver metastasis: potential impact on immune checkpoint inhibitor therapy. Eur Radiol 2019;29:5045-51.

[7] Solbiati L, Ahmed M, Cova L, Ierace T, Brioschi M, Goldberg SN. Small liver colorectal metastases treated with percutaneous radiofrequency ablation: local response rate and long-term survival with up to 10-year follow-up. Radiology 2012;265:958-68.

[8] Calandri M, Mauri G, Yevich S, Gazzera C, Basile D, Gatti M, et al. Fusion imaging and virtual navigation to guide percutaneous thermal ablation of hepatocellular carcinoma: a review of the literature. Cardiovasc Intervent Radiol 2019;42:639-47.

[9] Farouil G, Deschamps F, Hakime A, de Baere T. Coil-assisted RFA of poorly visible liver tumors: effectiveness and risk factors of local tumor progression. Cardiovasc Intervent Radiol 2014;37:716-22.

[10] Zheng X-H, Guan Y-S, Zhou X-P, Huang J, Sun L, Li X, et al. Detection of hypervascular hepatocellular carcinoma: comparison of multi-detector CT with digital subtraction angiography and Lipiodol CT. World J Gastroenterol 2005;11:200-3.
[11] van Tilborg AA, Scheffer HJ, Nielsen K, van Waesberghe JH, Comans EF, van Kuijk C, et al. Transcatheter CT arterial portography and CT hepatic arteriography for liver tumor visualization during percutaneous ablation. J Vasc Interv Radiol 2014;25:1101-11 e4.
[12] Piron L, Le Roy J, Cassinotto C, Delicque J, Belgour A, Allimant C, et al. Radiation exposure during transarterial chemoembolization: angio-CT versus cone-beam CT. Cardiovasc Intervent Radiol 2019;42:1609-18.
[13] Hermida M, Cassinotto C, Piron L, Assenat E, Pageaux GP, Escal L, et al. Percutaneous thermal ablation of hepatocellular carcinomas located in the hepatic dome using artificial carbon dioxide pneumothorax: retrospective evaluation of safety and efficacy. Int J Hyperthermia 2018;35:90-6.
[14] Kariya S, Tanigawa N, Kojima H, Komemushi A, Shomura Y, Ueno Y, et al. Radiofrequency ablation combined with CO2 injection for treatment of retroperitoneal tumor: protecting surrounding organs against thermal injury. AJR Am J Roentgenol 2005;185:890-3.
[15] de Baère T, Dromain C, Lapeyre M, Briggs P, Duret JS, Hakime A, et al. Artificially induced pneumothorax for percutaneous transthoracic radiofrequency ablation of tumors in the hepatic dome: initial experience. Radiology 2005;236:666-70.
[16] Deak PD, Smal Y, Kalender WA. Multisection CT protocols: sex- and age-specific conversion factors used to determine effective dose from dose-length product. Radiology 2010;257:158-66.
[17] Karavasilis E, Dimitriadis A, Gonis H, Pappas P, Georgiou E, Yakoumakis E. Dose coefficients for Liver chemoembolisation procedures using Monte Carlo code. Radiat Prot Dosimetry 2016;172:409-15.
[18] Cardella JF, Kundu S, Miller DL, Millward SF, Sacks D, Society of Interventional Radiology. Society of Interventional Radiology clinical practice guidelines. J Vasc Interv Radiol 2009;2:S189-91.
[19] Ahmed M, Solbiati L, Brace CL, Breen DJ, Callstrom MR, Charboneau JW, et al. Image-guided tumor ablation: standardization of terminology and reporting criteria - a 10-year update. J Vasc Interv Radiol 2014;25:1691-705.e4.

[20] Vietti Violi N, Duran R, Demartines N, Sempoux C, Guiu B, Bize PE, et al. Local recurrence rate in patients with colorectal cancer liver metastasis after wedge resection or percutaneous radiofrequency ablation. Int J Hyperthermia 2018;34:1020-8.
[21] Minami Y, Kudo M. Radiofrequency ablation of liver metastases from colorectal cancer: a literature review. Gut Liver 2013;7:1-6.
[22] Bing F, Vappou J, Breton E, Enescu I, Garnon J, Gangi A. Accuracy of a CT-Ultrasound fusion imaging guidance system used for hepatic percutaneous procedures. J Vasc Interv Radiol 2019;30:1013-20.
[23] Hakime A, Deschamps F, De Carvalho EG, Teriitehau C, Auperin A, De Baere T. Clinical evaluation of spatial accuracy of a fusion imaging technique combining previously acquired computed tomography and real-time ultrasound for imaging of liver metastases. Cardiovasc Intervent Radiol 2011;34:338-44.
[24] Volpi S, Tsoumakidou G, Loriaud A, Hocquelet A, Duran R, Denys A. Electromagnetic navigation system combined with high-frequency-jet-ventilation for CT-guided hepatic ablation of small US-undetectable and difficult to access lesions. Int J Hyperthermia 2019;36:1051-7.
[25] Soyer P, Bluemke DA, Fishman EK. CT during arterial portography for the preoperative evaluation of hepatic tumors: how, when, and why? AJR Am J Roentgenol 1994;163:1325-31.
[26] Soyer P, Bluemke DA, Hruban RH, Sitzmann JV, Fishman EK. Primary malignant neoplasms of the liver: detection with helical CT during arterial portography. Radiology 1994;192:389-92.
[27] Antoch G, Kuehl H, Vogt FM, Debatin JF, Stattaus J. Value of CT volume imaging for optimal placement of radiofrequency ablation probes in liver lesions: J Vasc Interv Radiol 2002;13:1155-61.
[28] Hermida M, Cassinotto C, Piron L, Aho-Glele S, Guillot C, Schembri V, et al. Multimodal percutaneous thermal ablation of small hepatocellular carcinoma: predictive factors of recurrence and survival in Western patients. Cancers 2020;12:313.
[29] Stattaus J, Kuehl H, Ladd S, Schroeder T, Antoch G, Baba HA, et al. CT-guided biopsy of small liver lesions: visibility, artifacts, and corresponding diagnostic accuracy. Cardiovasc Intervent Radiol 2007;30:928-35.

[30] Soyer P, Lacheheb D, Levesque M. False-positive CT portography: correlation with pathologic findings. AJR Am J Roentgenol 1993;160:285-9.
[31] Beregi JP, Greffier J. Low and ultra-low dose radiation in CT: Opportunities and limitations. Diagn Interv Imaging 2019;100:63-4.
[32] Zedira A, Greffier J, Brunet X, Pereira F, Winum PF, Granier M. Decreased operator X-ray exposure by optimized fluoroscopy during radiofrequency ablation of common atrial flutter. Diagn Interv Imaging 2018;99:625-32.
[33] Kloeckner R, dos Santos DP, Schneider J, Kara L, Dueber C, Pitton MB. Radiation exposure in CT-guided interventions. Eur J Radiol 2013;82:2253-7.
[34] Yang K, Ganguli S, DeLorenzo MC, Zheng H, Li X, Liu B. Procedure-specific CT dose and utilization factors for CT-guided Interventional procedures. Radiology 2018;289:150-7.
[35] Greffier J, Ferretti G, Rousseau J, Andreani O, Alonso E, Rauch A, et al. National dose reference levels in computed tomography-guided interventional procedures-a proposal. Eur Radiol 2020; doi: 10.1007/s00330-020-06903-9

FIGURE LEGENDS

Figure 1. Study flowchart. HCC indicates hepatocellular carcinoma.

Figure 2. Fifty-seven-year old woman with a single liver metastasis from colon cancer treated by radiofrequency thermal ablation under arterial CT portography guidance. A, CT image obtained during arterial portography in the axial plane shows subcapsular metastasis (arrow) at the hepatic dome, treated by radiofrequency thermal ablation under after creation of an artificial pneumothorax. B, Immediate post-treatment arterial CT-portography image shows the ablation zone (white arrow), which is markedly overestimated and the needle path (black arrow).

Figure 3. Thirty-nine-old woman with a single metastasis from colon cancer treated by radiofrequency ablation under arterial CT-portography guidance. A, CT image obtained during arterial portography in the axial plane shows small metastasis (arrow) at the hepatic dome, adjacent to middle hepatic vein. B, On immediate post-treatment arterial CT-portography image, the ablation zone (arrows) and segment I (arrowheads) appear hypoattenuating. C, Conventional CT image obtained during the portal phase immediately after radiofrequency ablation shows discordance regarding ablation zone assessment with smaller tumor ablation area size (arrows) and segment I with normal enhancement. D, E, At a upper level, on the same examinations than in B and C, arterial CT-portography image shows overestimation (arrowheads) of the ablation zone compared with conventional hepatic CT during the portal phase (E). It is assumed than differences in ablation area appearance may be due to portal venous flow disturbances induced by percutaneous ablation.

Table 1. Characteristics of hepatic tumors and percutaneous ablations.

Table 2. Radiation exposure during percutaneous ablation procedures.

Table 3. Radiation exposure during percutaneous tumor ablation of liver tumors using computed-tomography guidance in published studies.

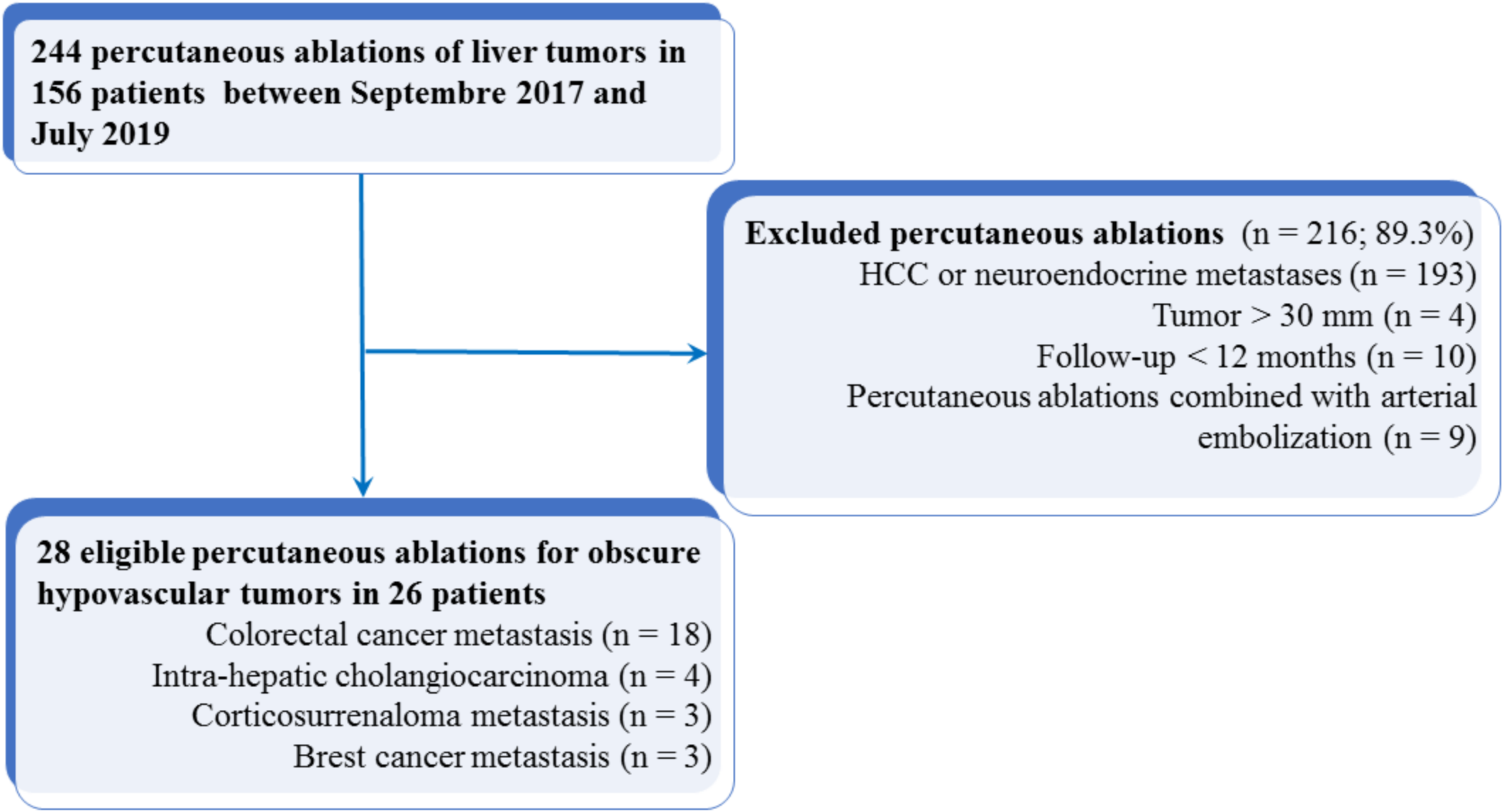
244 percutaneous ablations of liver tumors in 156 patients between Septembre 2017 and July 2019
Excluded percutaneous ablations (n = 216; 89.3%)
HCC or neuroendocrine metastases (n = 193)
Tumor > 30 mm (n = 4)
Follow-up < 12 months (n = 10)
Percutaneous ablations combined with arterial embolization (n = 9)
28 eligible percutaneous ablations for obscure hypovascular tumors in 26 patients
Colorectal cancer metastasis (n = 18)
Intra-hepatic cholangiocarcinoma (n = 4)
Corticosurrenaloma metastasis (n = 3)
Brest cancer metastasis (n = 3)

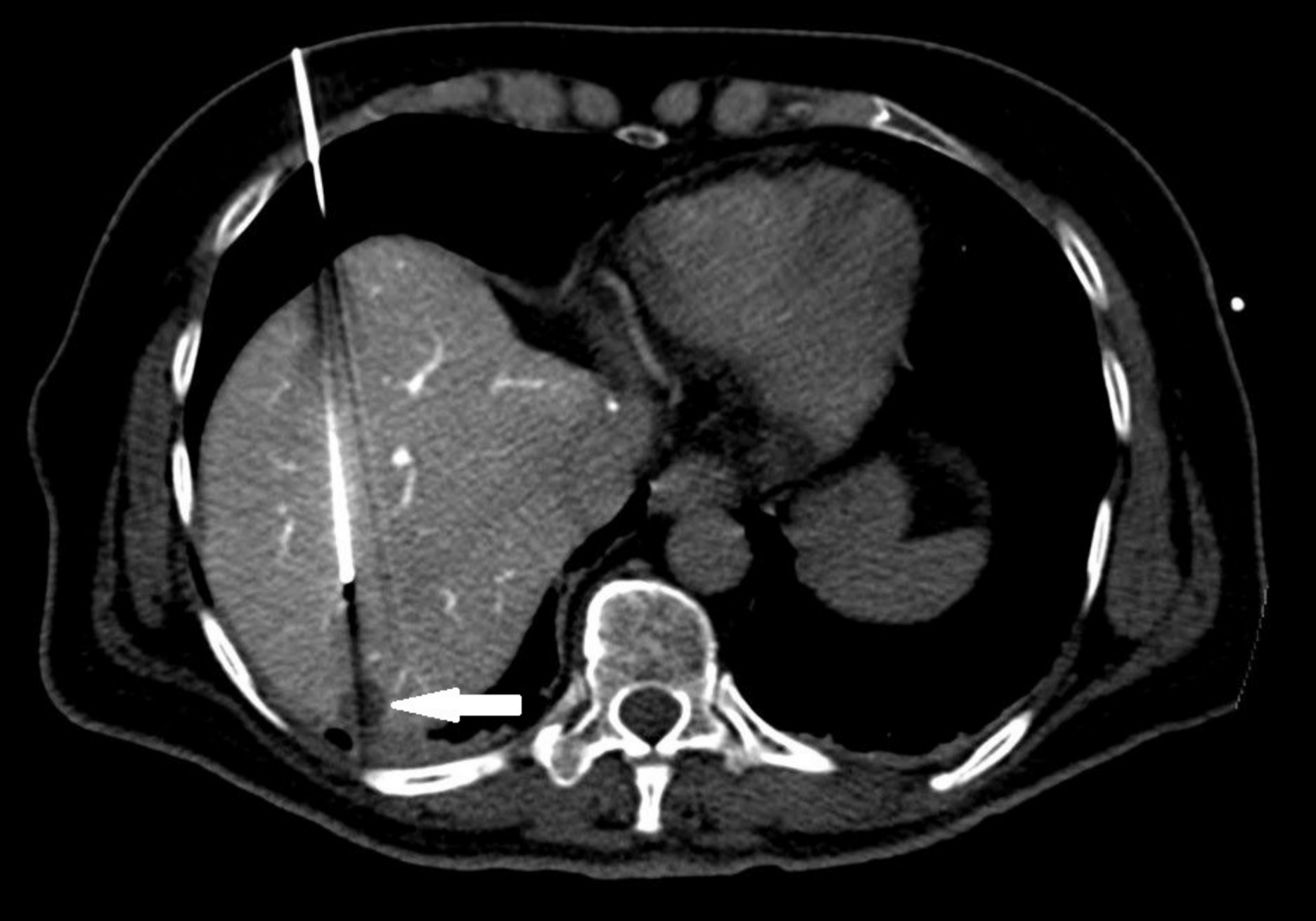

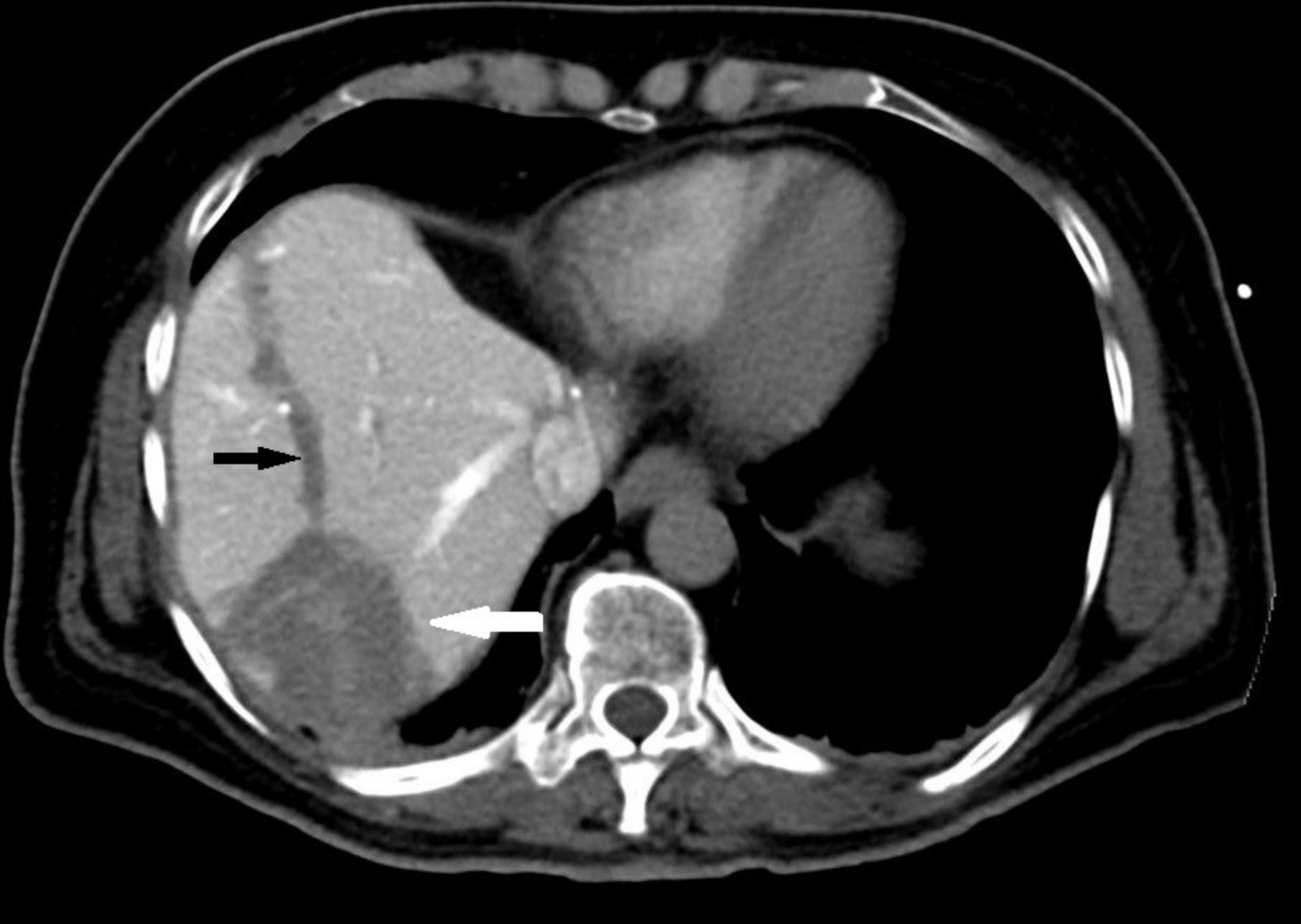

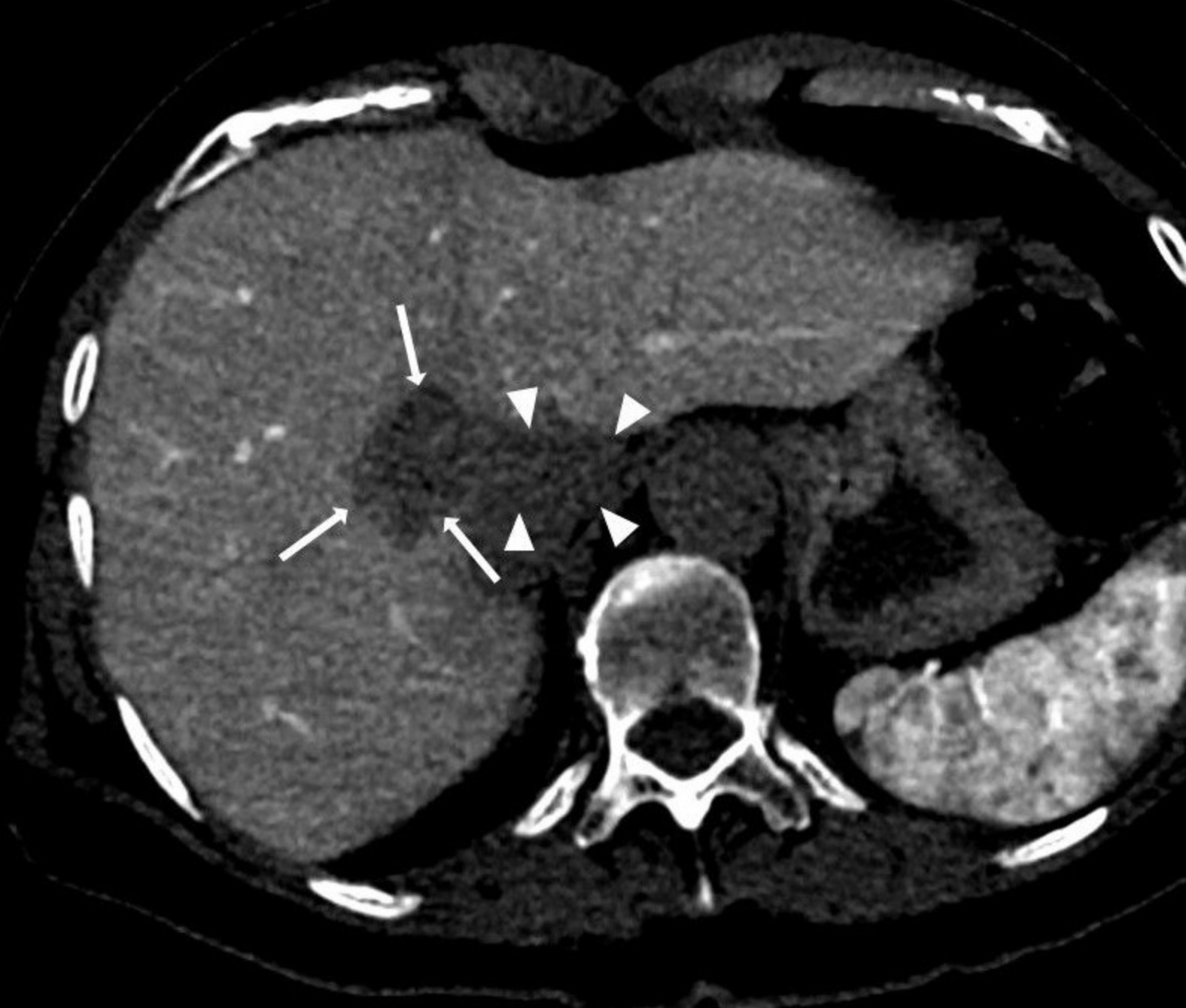

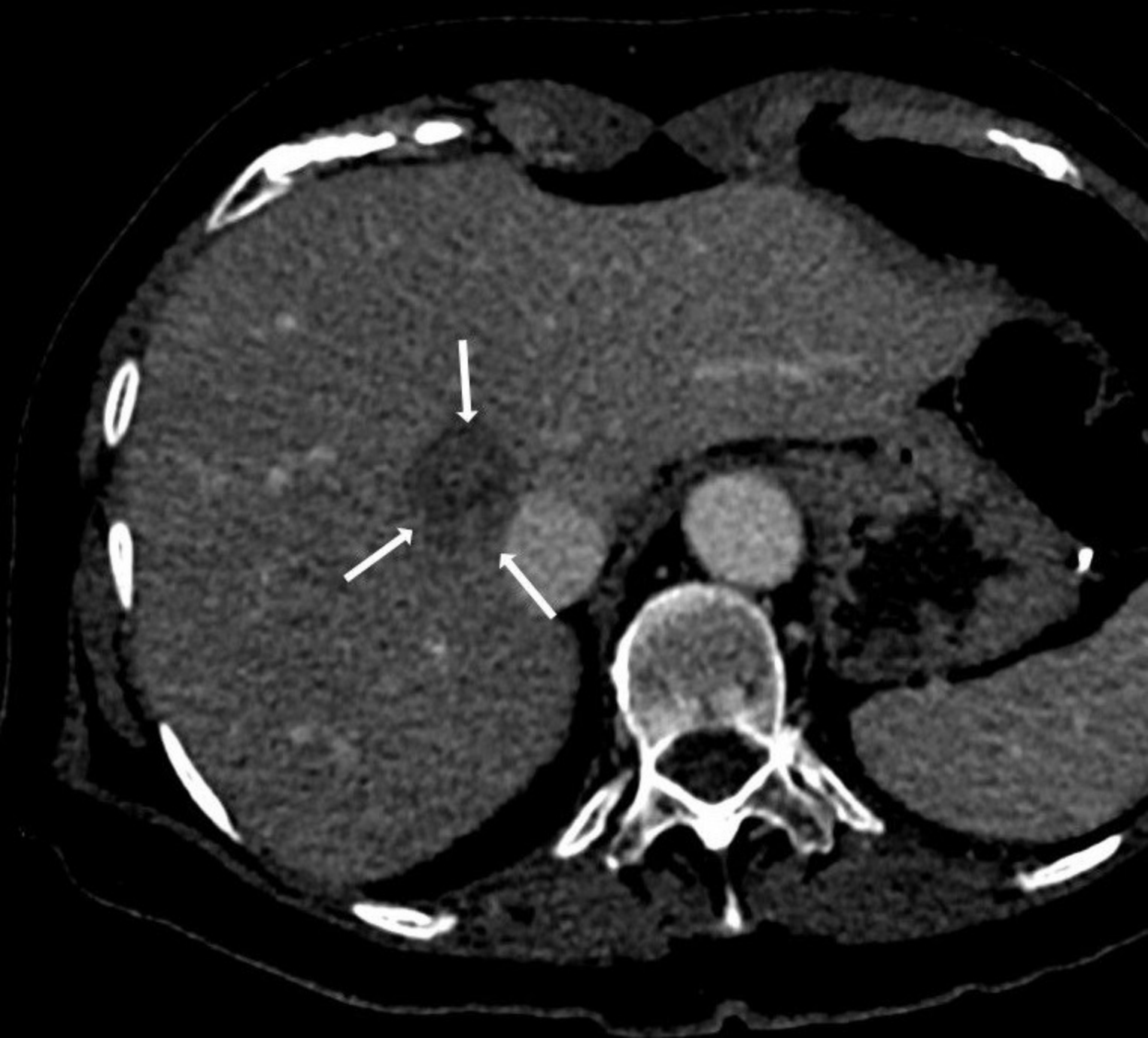

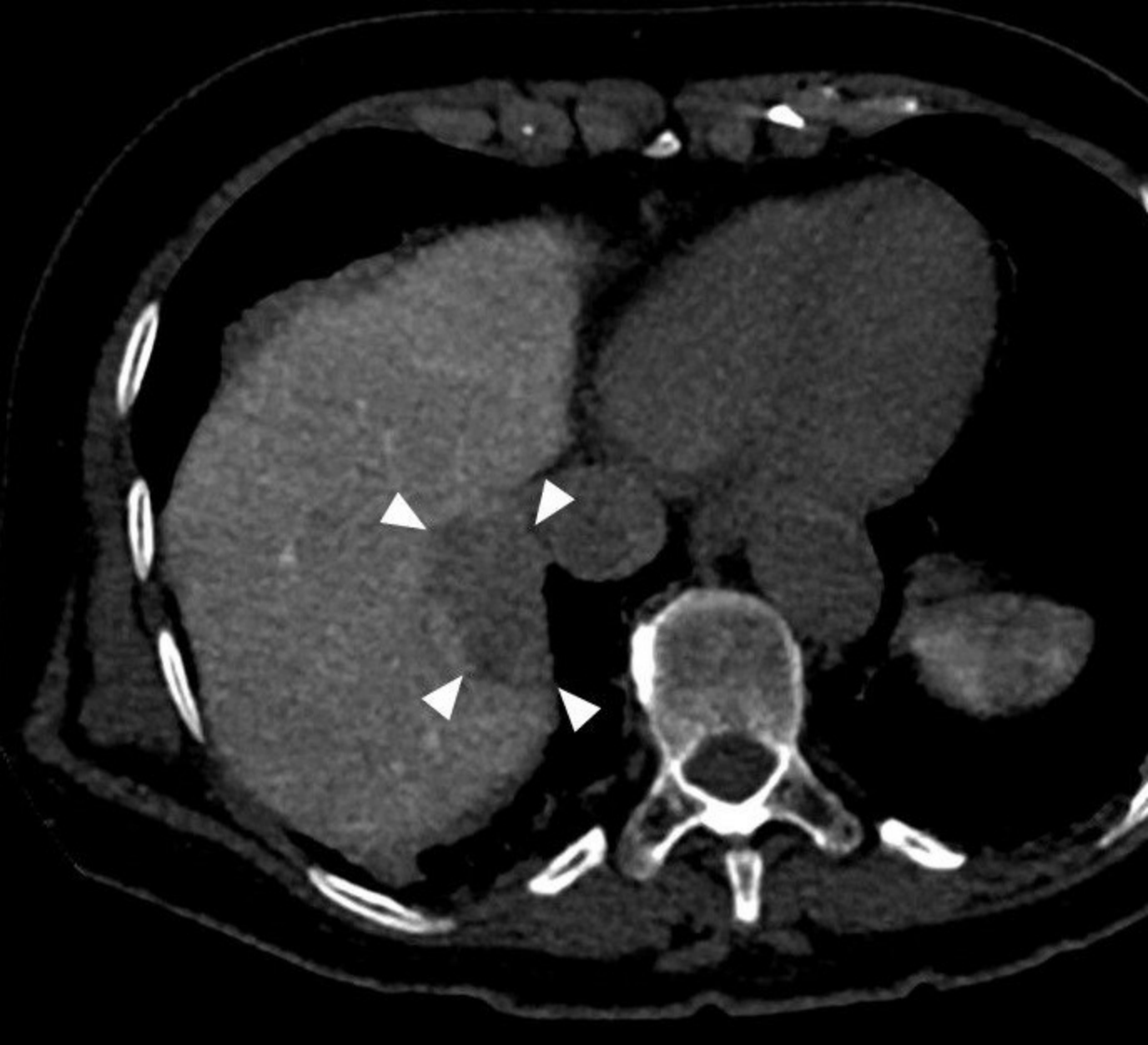

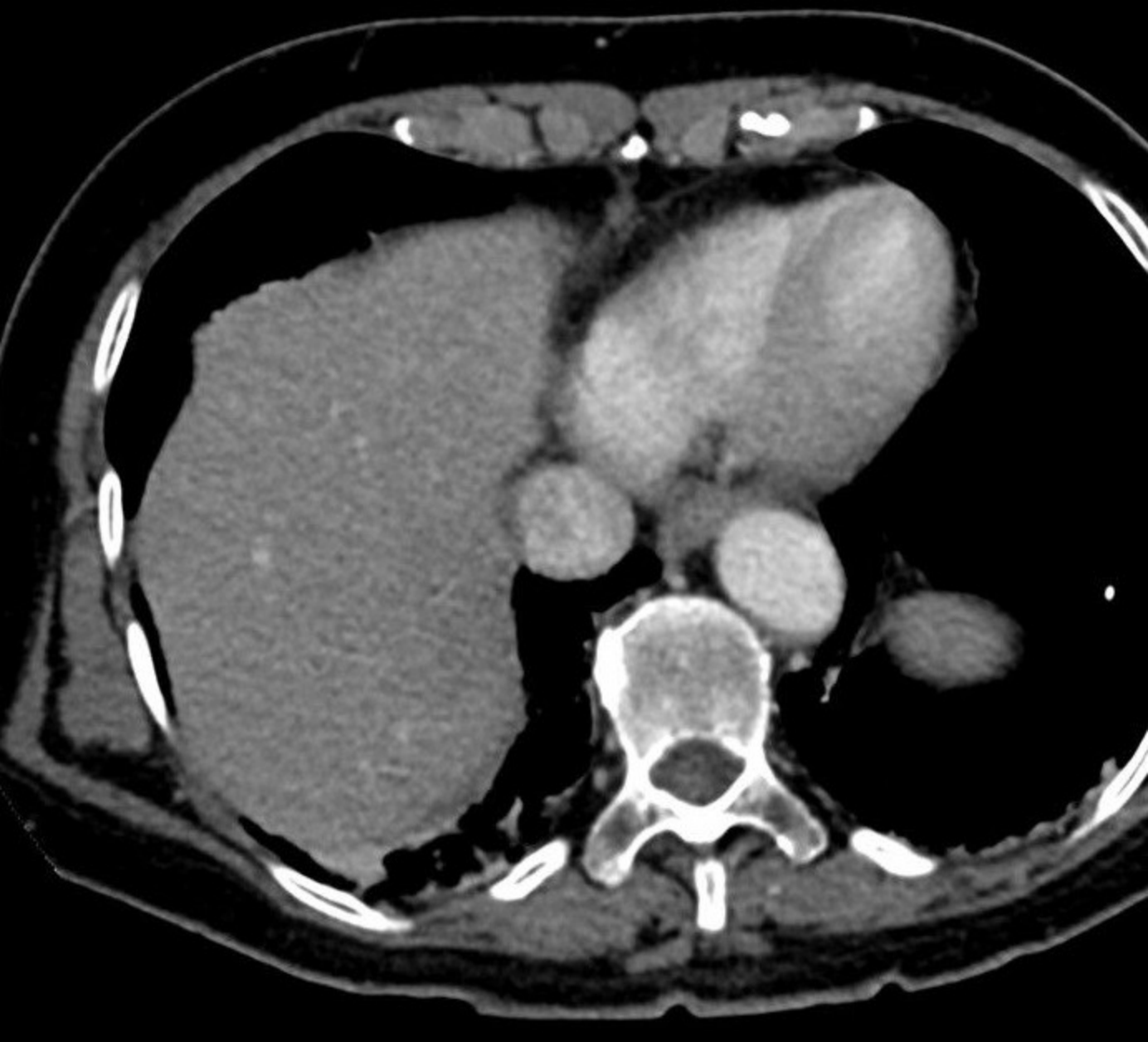

Tumor visibility on unenhanced CT	0 (0/28; 0%)
Tumor diameter (mm)	14 ± 10 [7 – 24]
Tumor type	
Metastasis from colon cancer	18 (18/28; 64%)
Intrahepatic cholangiocarcinoma	4 (4/28; 14%)
Corticosurrenaloma	3 (3/28; 11%)
Metastasis from breast cancer	3 (3/28; 11%)
Tumor location	
Dome	9 (9/28; 32%)
Subcapsular	14 (14/28; 50%)
Central	5 (5/28; 18%)
PTA modality	
Radiofrequency	12 (12/28; 43%)
Microwave	11 (11/28; 39%)
Irreversible electroporation	5 (5/28; 18%)
Additional techniques	
Artificial CO_2 pneumothorax	9 (9/28; 32%)
Hydro-dissection	3 (3/28; 11%)
Number of needles per tumor	2.5 ± 1.5 [1 – 5]
Technical success	28 (28/28; 100%)
Local tumor progression	2 (2/28; 7%)

Quantitative data are expressed as means ± standard deviations; , numbers in brackets are ranges. Qualitative data are expressed as raw numbers; numbers in parentheses are percentages followed by percentages.

CT = Computed tomography; PTA = Percutaneous thermal ablation; CO_2 = Carbon dioxide

CT		2D angiography		Total
Dose-length product (mGy.cm)	**Effective dose (mSv)**	**Dose-area product (Gy.cm²)**	**Effective dose (mSv)**	**Effective dose (mSv)**
1727 ± 547 [1260 – 2125]	25.9 ± 8.2 [18.9 - 31.9]	1.68 ± 0.82 [0.89 – 1.99]	0.27 ± 0.13 [0.14 – 0.32]	26.5 ± 8.2 [19.1 – 32.2]

Values are expressed as means standard ± deviation median; numbers in brackets are ranges
CT = computed tomography; 2D = two-dimensional;

Reference	Technique	DLP (mGy.cm) : Median (Q1; Q3)
Greffier et al. 2020 [33]	RFA/MWA	**1535 (990; 2461)**
Yang et al. [32] 2018	RFA/MWA	**2351 (1612; 3405)**
Kloeckner et al. [31] 2013	RFA/MWA	**1403 (N.A.; 1906)**
This study	RFA/MWA/IRE	**1717 (1257; 2138)**

RFA: Radiofrequency ablation; MWA: Microwave ablation; IRE: Irreversible electroporation; NA: Not available
Data are expressed as medians; numbers in parentheses are first quartiles followed by third quartiles